**CAAP Quarterly Report**

Date of Report: <*July* 10th, 2018>

Contract Number: <DTPH56-15-H-CAAP06>

Prepared for: <Government Agency: U. S. DOT PHMSA >

Project Title: <*Mitigating Pipeline Corrosion Using A Smart Thermal Spraying Coating System*>

Prepared by: <North Dakota State University>

Contact Information: <Dr. Fardad Azarmi, Email: fardad.azarmi@ndsu.edu, Phone: 701.231.9784; Dr. Ying Huang, Email: ying.huang@ndsu.edu, Phone: 701.231.7651.>

For quarterly period ending: <*July* 10th, 2018>

<u>**Business and Activity Section**</u>

**(a) Generated Commitments**

No changes to the existing agreement.

No equipment purchased over this reporting period.

No supplies purchased in this quarter.

**(b) Status Update of Past Quarter Activities**

In this quarter, studies were mainly focused on conducting numerical analysis on cold sprayed Al-Zn coatings, mechanical tests on wire arc sprayed coatings, and full-size pipe experiments to locate and identify corrosion on soft coating coated pipes using FBG sensors. The details of this quarter report includes: 1) finite element analysis (FEA) on cold sprayed Al-Zn coating; 2) mechanical test results on wire arc sprayed Al-Zn coating; 3) preparing the full-size pipe sample with soft coating and hard coating; and 4) test results and data analysis on soft coated full-size pipe experiments. The corrosion location was successfully identified in the multiple sensor setup. Further efforts would be put on continuing conduct the proof-of-concept experiments on hard coatings and multi-layer coatings. The detailed progresses could be found below:

    1) <u>Finite element analysis on cold sprayed Al-Zn coating</u>

In last quarter report (the tenth quarter report), wire arc sprayed coatings were evaluated using finite element analysis on the actual micrographs of the coating using image analysis by Object

Oriented Finite (OOF) element to better understand the influence of the microstructural features (such as voids, pores, and splat boundaries) on the mechanical and physical properties of the coating. As an alternative approach to coating deposition, cold spraying technology was employed to deposit coatings with the same material Al-15Zn. The cold spraying technology heated the coating powders to a semi-molten state and shot towards the substrate at a speed of up to 1200 m/s. This technology is one the newest members of thermal spraying techniques and it can produce high quality coatings consisting of low porosities. As discussed in the previous report, OOF will be used to perform FEA on micrographs of cold sprayed coating.

*Image Analysis FEA Process Using OOF:* After completing the metallography process on the cold sprayed coating samples, several micrographs were taken from randomly selected positions along the cross-section of the cold sprayed coating using optical microscopy. Figure 1 shows an optical micrograph of the as-sprayed coating.
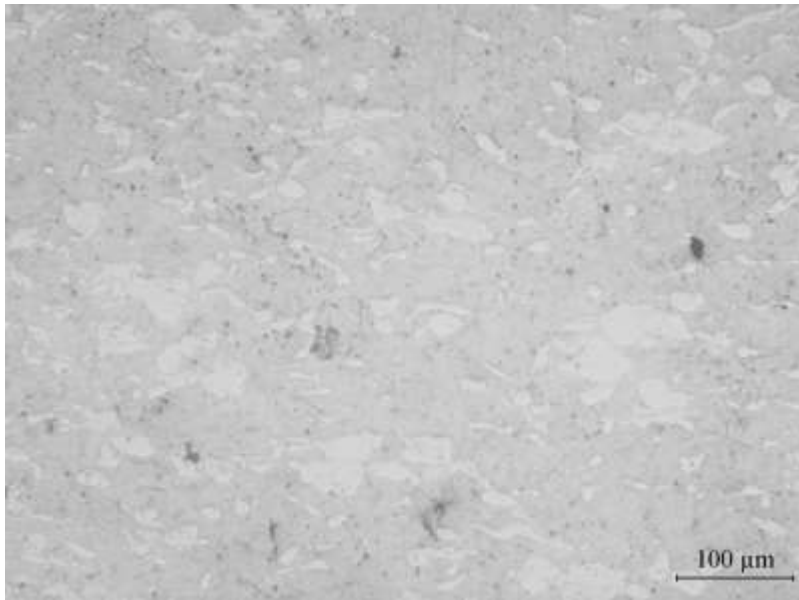


Figure 1. Optical microscopic image of Al-15Zn cold sprayed coating cross-section.

According to Figure 1, there are three different regions on the microstructure of the coating consisting of voids (black), zinc (light gray), and aluminum (dark gray). Therefore, three different groups are created and pixels from each region are added to their corresponding group. As mentioned in the earlier report, pixels are selected based on their contrast using RGB method in Pixel Selection menu. Table 1 shows the number of pixels and percentage of each group.

Table 1. Number of pixels and percentage of each group

| Group | Number of Pixels | Percentage |
|-------|------------------|------------|
| Al | 2322188 | 80.61 |
| Zn | 525085 | 18.22 |
| Pores | 33681 | 1.17 |
| Total | 2880800 | 100 |

In the materials menu, values of E and ν are determined for each group based on the values from Table 2. Since the elastic modulus cannot be set to zero, a really small number such as 1×e-9 GPa, is assumed for the elastic modulus of voids and pores.

Table 2. Mechanical properties of different regions for Al-15Zn cold sprayed coating

| Group | E $(GPa)$ | ν |
|-------|-----------|---|
| Al | 70 | 0.34 |
| Zn | 100 | 0.25 |
| Pores | 10-9 | 0.3 |

Then, colors are assigned to each group to properly distinguish them from one another. Figure 2 shows the modified image.
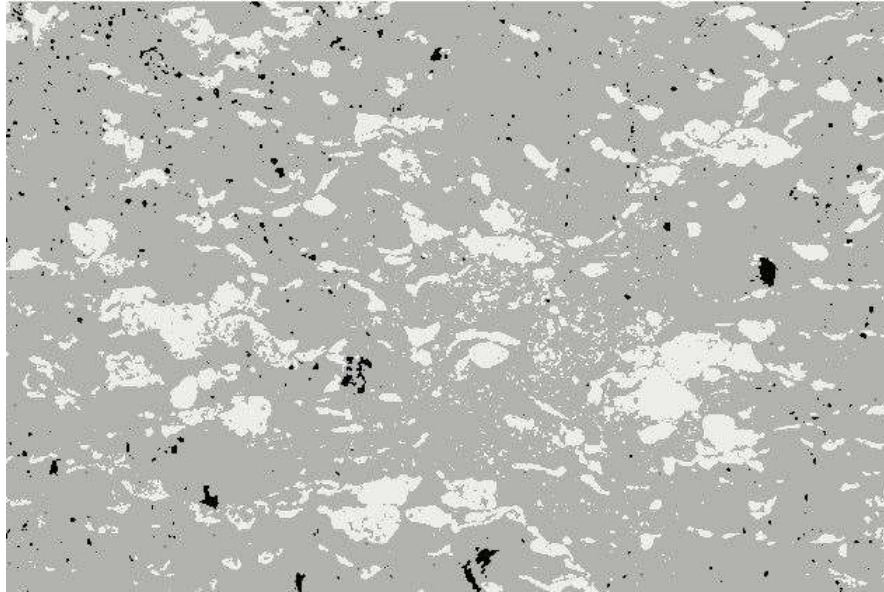


Figure 2. Modified image: black, dark, and light pixels representing voids, aluminum, and zinc, respectively.

In the next step, elements are created based on the modified image and produced an elemental structure for numerical simulation consisted of 210 x-elements and 140 y-elements. This

skeleton is further modified to increase the homogeneity of elements. Modification process includes smooth, snap anneal, and snap refine which is shown in Figure 3. The final skeleton reached a homogeneity of 0.982.

The OOF method can solve a Force Balance problem with defined boundary conditions and displacements. Fixed boundary is considered for the left side of the image, while displacement is applied on the opposite side of the image. Considering, the strain at yielding and Young's modulus of both pure aluminum and zinc, a displacement of 0.0002 would be satisfactory to avoid yielding of the coating. As for top and bottom of the image, boundary conditions are set free. After solving the problem, the OOF can report average values of stress and strain over the entire mesh shown. Average values of stress and strain in x-direction are shown in Figure 4.



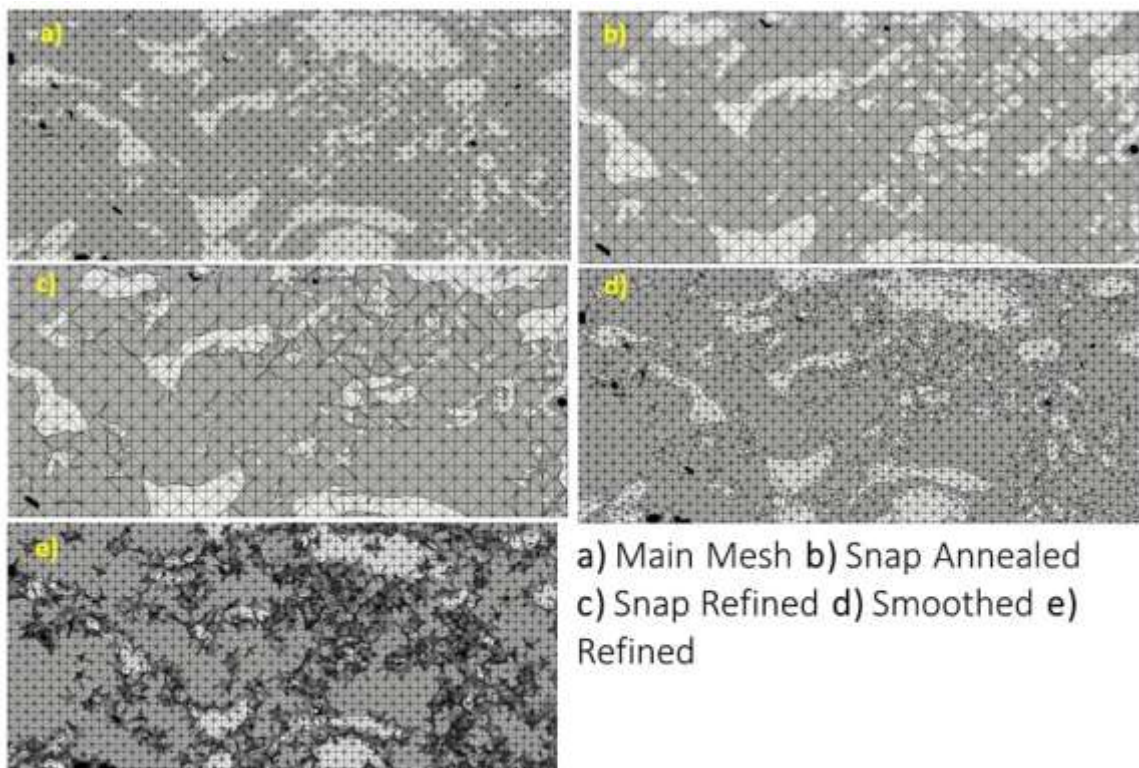a) Main Mesh b) Snap Annealed c) Snap Refined d) Smoothed e) Refined

Figure 3. Image modification process.

```
# Operation: Average and Deviation
# Output: Geometric Strain[xx]
# Domain: EntireMesh
# Sampling: ElementSampleSet(order=automatic)
# Columns:
# 1. time
# 2. average of Geometric Strain[xx]
# 3. standard deviation of Geometric Strain[xx]
0.0, 9.61538461538e-08, 2.83474693705e-07

# Operation: Average and Deviation
# Output: Stress[xx]
# Domain: EntireMesh
# Sampling: ElementSampleSet(order=automatic)
# Columns:
# 1. time
# 2. average of Stress[xx]
# 3. standard deviation of Stress[xx]
0.0, 7.6482643062e-06, 1.61843833634e-06
```

Figure 4. Average values of stress and strain reported by OOF.

By substituting the average values into Equation (1), the Young's modulus of the cold sprayed Al-15Zn coating can be estimated using object oriented finite element analysis.

$$E = \frac{\sigma_{xx}(1 - \vartheta)}{\varepsilon_{xx}} = 53.8499 \; GPa \tag{1}$$

It should be noted that Equation (1) can be reorganized to find an average value of Poisson ratio as in Equation (2) below:

$$\vartheta = \frac{A_{Al}\vartheta_{Al} + A_{Zn}\vartheta_{Zn}}{A_{Al} + A_{Zn}} = 0.323 \tag{2}$$

To achieve more accurate results for estimating the elastic modulus of the coating, this process is repeated for other randomly taken micrographs over the coating. Table 3 lists the results of analysis on two different micrographs which indicates that Al-Zn coating is weaker than zinc or aluminum in terms of elastic modulus, yet it has shown better properties than the wire arc coating analysis performed in the previous report.

Table 3. OOF results on two different micrographs

| Group | Average Strain | Average Stress | Elastic Modulus (GPa) |
|---|---|---|---|
| Micrograph I | 9.6153e-08 | 7.6482e-06 | 53.8499 |
| Micrograph II | 1.4367e-07 | 1.1505e-05 | 54.0544 |

2) <u>Mechanical experiments on wire arc sprayed Al-Zn coating</u>

In the previous report, the elastic properties of wire arc sprayed samples were investigated using finite element simulations and numerical analysis. In this report, the goal is to find out the mechanical behaviors of the coating under different experimental tests. Both wear and hardness test were carried out and results are discussed in this report. Wear test determine the behavior of the coating in physical contact with other objects which may result in friction and abrasion and material loss over time. Hardness test can show the resistance of the coating to any indentation and deformation.

The wear test is performed in the UMT DFH20G Bruker machine, which can apply force up to 200 N. This device can measure Sliding Wear and Friction Behavior between a Static Pin (Area Contact) or Ball (Point Contact) and a Rotating Surface. For this experiment, the indenter applies a load of 10 N, rotating on a circle with a diameter of 2 cm at 265 rpm for 80 min, corresponding to a total distance of 1,332 m.

The hardness test was carried out using a Rockwell tester at load of 100 kgf and a steel ball with a diameter of 1.588 mm. Rockwell is a fast method, developed for production control and it has a direct readout. Because of the effects of the corrosion and the wear tests on the coating, there are three regions on the sample, outside of the glued region (R1), inside of the glued region (R2), and the worn-out region (R3) caused by the wear test. The hardness test was performed on each region. Figure 5 shows different regions of sample under hardness test.
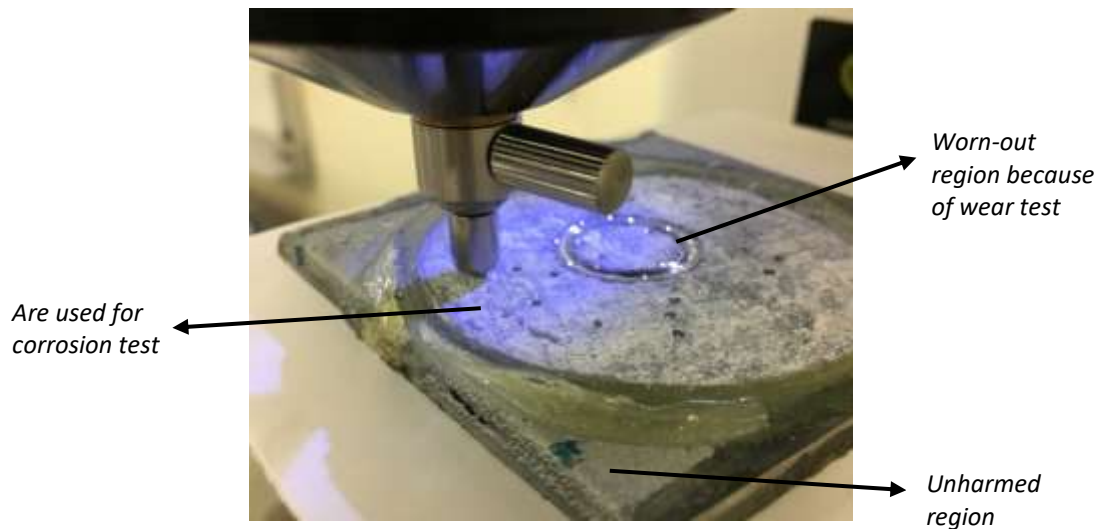


Worn-out region because of wear test

Are used for corrosion test

Unharmed region

Figure 5. Regions used for hardness test.

Table 4. Coefficient of friction resulted from wear test on Al-15Zn wire arc coating

| Surface of Wear Test | Fx | Fz | COF |
|---|---|---|---|
| Al-Zn Coating | 4.186±1.018 | 10.18±1.787 | 0.4121±0.071 |
| Aluminum Substrate | 4.87±0.6088 | 9.966±0.635 | 0.4883±0.501 |

Table 5. Hardness test results of Al-15Zn wire arc coating – Rockwell scale B (HRB)

| Number of Test | R1 | R2 | R3 |
|---|---|---|---|
| 1 | 41.8 | 24.8 | 42.7 |
| 2 | 47.1 | 24.6 | 31.9 |
| 3 | 43.9 | 35 | 51.3 |
| 4 | 49.1 | 38.5 | 47.7 |
| 5 | 47.3 | 21.4 | 38.8 |
| 6 | 51.2 | 37.2 | 40.1 |
| 7 | 56.7 | 38.6 | 38.7 |
| 8 | 56.3 | 27.5 | 39.5 |
| Average | 49.17±5.36 | 30.95±7.09 | 41.33±5.96 |

The results of wear test show an improvement of the surface after applying the Al-15Zn wire arc coating as coefficient of friction has dropped and causes less material damage and loss over certain period of time. On the other hand, hardness test results imply that R2 which suffers from salts caused by corrosion test has less hardness than aluminum, while R1 which is as-deposited coating has better hardness behavior compared to bare aluminum. Considering the results of both tests, it can be concluded that applying Al-15Zn wire arc coating improved mechanical properties of the surface.

In future studies, it is aimed to conduct wear and hardness tests on cold sprayed Al-15Zn coating and compare them with results of wire arc deposited coating.

3) Sample preparation for full-size experiments on corrosion in soft coatings

On the other hand, to locate the corrosion on a steel pipe, more than three FBG sensors are estimated to be needed and they should not be on a straight line. Thus, in the full-size pipe teste, a total of four sensors were embedded in the samples with soft coating (tested in this quarter, shown in Figure 6 and samples with hard coating which to be reported in next quarter.
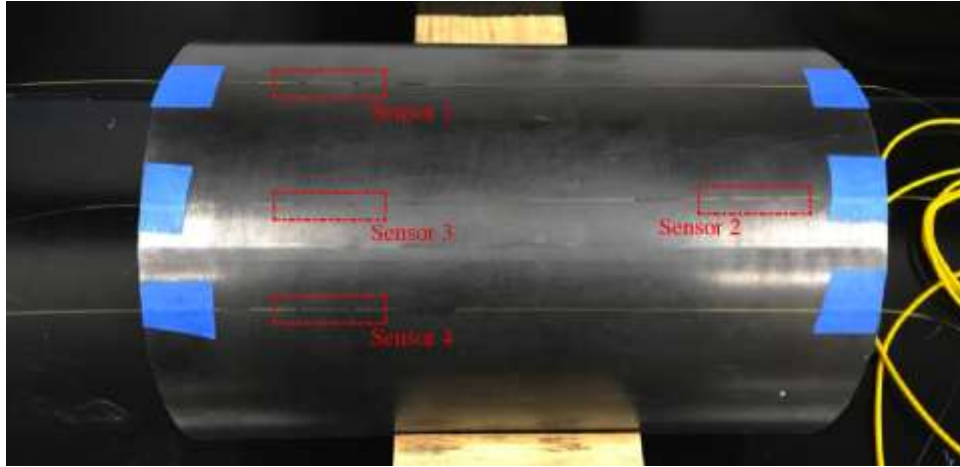
Figure 6. Steel pipe sample embedded with four FBG sensors.

In Figure 6, the blue tapes were only used for fixing the location of FBG sensors, and since they were on the edge of the pipe and not going to react chemically with other material, they would not affect the testing environment.

After applying the soft coating on the surface of the pipe as shown in Figure 6, the pipe was placed in sand with 20% moisture content. The sand fully covered the pipe to simulate the real application environment and the FBG sensors were connected to integrator for data collection as shown in Figure 7 and Figure 8.


Figure 7. Steel pipe sample coated with soft coating being put in box filled with sand.

Figure 8. Experiment setup for the steel pipe sample coated with soft coating.

The distances between four embedded sensors were shown in Figures 9 to 11. The distance between Sensor 1 and Sensor 3 is 2 inches, Sensor 2 and Sensor 3 is 7 inches, and Sensor 3 and Sensor 4 is 1.75 inches.



Figure 9. Distance measurement between Sensor 2 and Sensor 3.

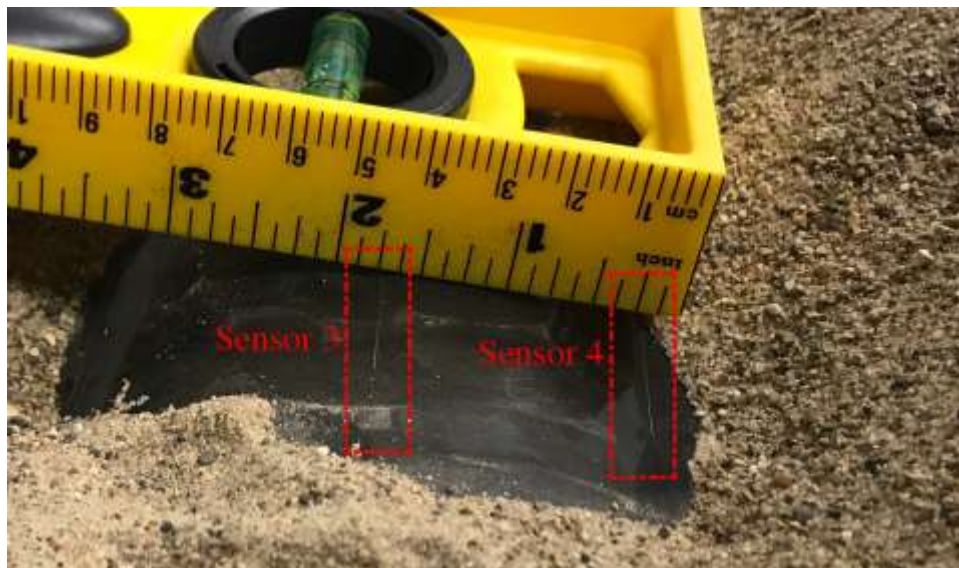Figure 10. Distance measurement between Sensor 1 and Sensor 3.


Figure 11. Distance measurement between Sensor 3 and Sensor 4.

4) Data analysis for full-size pipe corrosion experiments on soft coatings

Temperature sensor was located in sand to compensate the temperature effect on FBG sensors. Experiment was started at 2:00pm on May 14th, 2018 and ended at 8:00am on Jun 20th, 2018, which had a total duration of 882 hours. In order to accelerate the corrosion and emulate the coating crack damage, a crack of 0.75 inch in length was made near Sensor 3 around 11:00am on Jun 12th, 2018. The crack location was shown in Figures 12 to 14.

Figure 12. A crack is intentionally made to mock the actual crack happened on coating.


Figure 13. Distance measurement between crack and Sensor 2/Sensor 3.


Figure 14. Distance measurement between crack and Sensor 1/Sensor 3.

The collected data was shown in Figure 15. After temperature compensation, all data collected by the four FBG sensors were has also shown in Figure 16. It can be seen that a dramatic wavelength drop after crack was made on the soft coating, which was expected as our previous results have proven the same effect for multiple times. In addition, after the initial sudden drop the lowest wavelength change value varied from Sensor 1 to Sensor 4. As Sensor 3 had the

lowest wavelength change value (highest in absolute value), Sensor 1 and Sensor 4 had the second lowest wavelength change value and their value were close to each other, and Sensor 2 had the highest wavelength change value (lowest in absolute value). All these values variations could serve as an indicator to locate the corrosion. By combining the longitudinal and transverse distance from the crack to each sensor, the straight-line distance between the crack and distance could be found, which are 2.03 inches, 6.01 inches, 1.07 inches, and 2.37 inches for Sensor 1 to 4, respectively. The wavelength changes as shown in the graph, could confirm that corrosion was occurred near Sensor 3. The distances from corrosion to Sensor 1 and Sensor 4 are similar to each other and the corrosion is located further from Sensor 2 due to the lowest absolution wavelength change value.
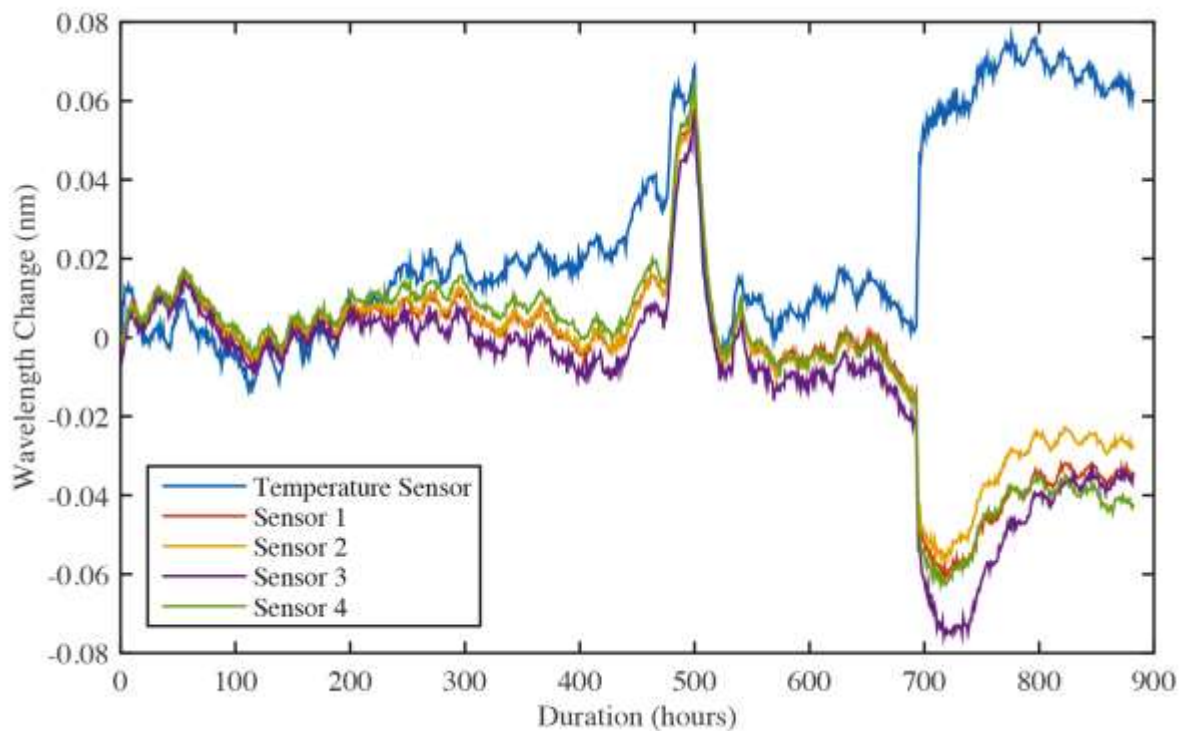


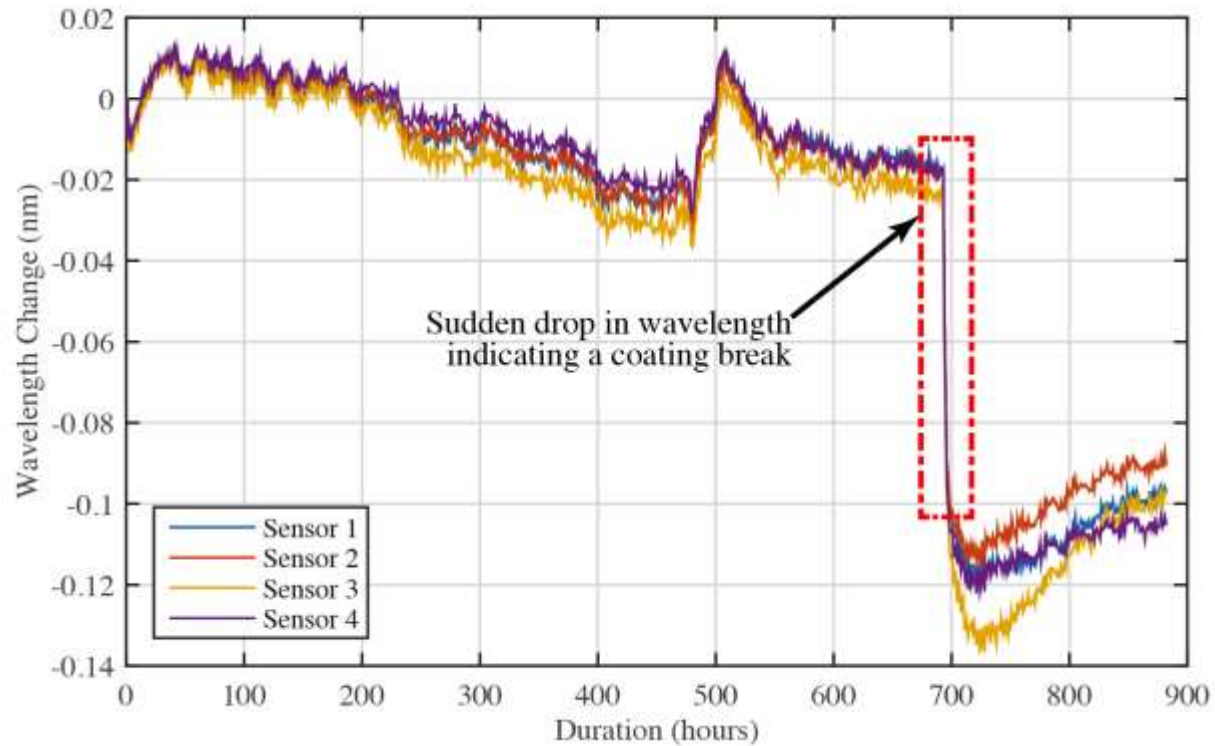Figure 15. Data collected by FBG sensors before eliminating the temperature effect.

Figure 16. Data collected by FBG sensors after eliminating temperature effect.

### (c) Description of Problems/Challenges

No problems observed in this quarter.

### (d) Planned Activities for the Next Quarter

The planned activities for next quarter are listed as below:
1) Sensor networking and corrosion damage characterization (Task 3.2);
2) Experiments for cold sprayed coating (Task 2.5);
3) Full-size experimental tests to localize corrosion on both hard coatings and multi-layer coatings through embedded sensor network (Task 4.2).